Surface Enrichment of Surfactants in Amorphous Drugs: An X-Ray Photoelectron Spectroscopy Study

Junguang Yu¹, Yuhui Li¹, Xin Yao¹, Chailu Que², Lian Huang², Ho-Wah Hui², Yuchuan Gong,^{2,3} Feng Qian,⁴ Lian Yu^{1,5,*}

Abstract:

Surfactants are commonly incorporated into amorphous formulations to improve the wetting and dissolution of hydrophobic drugs. Using X-ray photoelectron spectroscopy (XPS), we find that a surfactant can significantly enrich at the surface of an amorphous drug, up to 100 % coverage, while maintaining bulk miscibility. We compared four different surfactants (Span 80, Span 20, Tween 80, and Tween 20) in the same host acetaminophen and the same surfactant Span 80 in four different hosts (acetaminophen, lumefantrine, posaconazole, and itraconazole). For each system, the bulk concentrations of the surfactants were 0, 1, 2, 5, and 10 wt %, which cover the typical concentrations in amorphous formulations, and component miscibility in the bulk was confirmed by DSC. For all systems investigated, we observed significant surface enrichment of the surfactants. For acetaminophen containing different surfactants, strongest surface enrichment occurred for the most lipophilic Span 80 (lowest HLB), with nearly full surface coverage. For the same surfactant Span 80 doped in different drugs, the surface enrichment effect increases with the hydrophilicity of the drug (decreasing $\log P$). These effects arise because low-surface-energy molecules (or molecular fragments) tend to enrich at a liquid/vapor interface. This study highlights the potentially large difference between the surface and bulk compositions of an amorphous formulation. Given their high mobility and low glass transition temperature, the surface enrichment of surfactants in an amorphous drug can impact its stability, wetting, and dissolution.

Keywords: amorphous drug; surfactant; surface characterization; XPS; surface enrichment

Corresponding Author

*E-mail: lian.yu@wisc.edu

¹ School of Pharmacy, University of Wisconsin-Madison, Madison, WI 53705, USA

² Drug Product Development, Bristol Myers Squibb, 556 Morris Avenue, Summit, NJ 07901, USA

³ Small Molecule CMC, BeiGene (Beijing) Co., Ltd., Beijing 102206, China

⁴ School of Pharmaceutical Sciences and Beijing Advanced Innovation Center for Structural Biology, Tsinghua University, Beijing 100084, China

⁵ Department of Chemistry, University of Wisconsin-Madison, Madison, WI 53705, USA

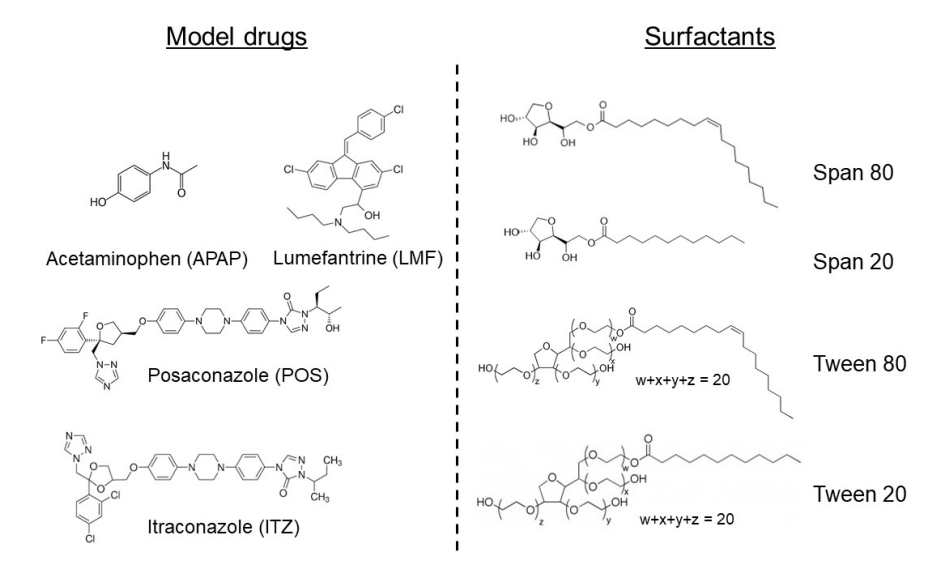
Introduction

Amorphous Solid Dispersion (ASD) is a widely used technology to enhance the solubility and bioavailability of poorly soluble drugs.¹ A typical ASD contains a drug, a polymer and a surfactant. With a typical concentration of 5–10 wt %, the surfactant facilitates the wetting and dissolution of the usually hydrophobic drug² and serves as a plasticizer to lower the processing temperature of hot melt extrusion (HME).³

A surfactant is known to enrich at the surface of an aqueous solution. In this process, the surfactant's hydrophobic tail is excluded from water and its hydrophilic head remains in contact with the aqueous medium, thus lowering the surface energy of the system.⁴ Although the surface enrichment effect has been extensively studied for surfactants in aqueous solutions, the phenomenon is less well understood for surfactants in hydrophobic solvents where the solvent also has low surface energy and thus competes with the surfactant for surface enrichment.^{5, 6} To our knowledge, the surface enrichment effect has never been studied for surfactants in ASDs.

The need to understand whether a surfactant is enriched at the surface of an ASD is highlighted by the recent finding⁷ that molecules can be extremely mobile at the surface of amorphous drugs. This high surface mobility in turn leads to fast surface crystallization^{8, 9} and failure of the amorphous formulation. Given that common pharmaceutical surfactants have high mobility and low glass transition temperature T_g , ¹⁰ their enrichment at the surface of ASDs would increase local mobility and accelerate crystallization. The surface enrichment of surfactants is also expected to alter the wetting and dissolution characteristics of the ASD.

In this study we utilized X-ray photoelectron spectroscopy (XPS)¹¹⁻¹³ to investigate the surface enrichment effects of surfactants in amorphous drugs. Scheme 1 and Table 1 show the drugs and surfactants used in this study. Four common pharmaceutical surfactants (Span 80, Span 20, Tween 80, and Tween 20) were studied. These surfactants have systematically changing structures. For example, Span 80 and Tween 80 have the same hydrophobic tail but Tween 80 has a larger hydrophilic head group; Span 80 and Span 20 have the same hydrophilic head but Span 80 has a longer hydrophobic tail. We compare the four surfactants in the same host acetaminophen (APAP), as well as the same surfactant Span 80 in four different drug hosts (acetaminophen, lumefantrine, posaconazole, and itraconazole). The surfactant concentrations used (0–10 wt %) cover the typical concentrations in ASDs, and component miscibility in the bulk was confirmed by DSC. For all systems investigated, we observed significant surface enrichment of the surfactants. For different surfactants doped in acetaminophen, strongest surface enrichment occurred for the most lipophilic Span 80 (lowest HLB), with its surface concentration approaching 100 %. For the same surfactant Span 80 doped in different drugs, the surface enrichment effect increases with the hydrophilicity of the drug (decreasing log P). These effects are explained by the tendency for component segregation at the liquid/vapor interface to minimize surface energy. Our results highlight the potentially large difference between the surface composition and the bulk composition of an ASD. Given their high mobility and low $T_{\rm g}$, the surface enrichment of surfactants can potentially accelerate surface crystallization and alter the wetting and dissolution of amorphous particles.



Scheme 1. Model drugs and surfactants used in this study.

Table 1. Physical properties of the drugs and surfactants used in this study

Compound	Formula	T _g onset (K)	$\log P$
Acetaminophen (APAP, pain medicine)	C8H9NO2	294	0.46^{14}
Lumefantrine (LMF, antimalarial)	$C_{30}H_{32}Cl_3NO$	292	$2.9^{15, 16}$
Posaconazole (POS, antifungal)	$C_{37}H_{42}F_2N_8O_4$	332	4.77^{17}
Itraconazole (ITZ, antifungal)	C35H38Cl2N8O4	330	5.66^{18}

Surfactant	Formula	HLB	1
Span 80	C24H44O6	4.3	Most lipophilic
Span 20	$C_{18}H_{34}O_6$	8.6	
Tween 80	C64H124O26	15	
Tween 20	C58H114O26	16.7	Most hydrophilic

^aHLB: Hydrophilic-Lipophilic Balance. The values are from Ref. 19.

Experimental Section

Materials

Acetaminophen (APAP, 99.0 %) was purchased from Sigma-Aldrich (St. Louis, MO). Itraconazole (ITZ, 98 %) was purchased from Alfa Aesar (Ward Hill, MA). Posaconazole (POS) was a gift from Merck (Kenilworth, NJ). These three drugs were used as received. Lumefantrine (LMF, 97 %) was purchased from Nanjing Bilatchem Industrial Co. (Nanjing, China) and used after re-crystallization from CH₂Cl₂ solution. Surfactants Span 20, Span 80, Tween 20 and Tween 80 were obtained from Sigma-Aldrich (St. Louis, MO) and used as received.

Sample preparation

200 mg total of a drug containing 10 wt % or 20 wt % surfactant was mixed by grinding with 0.4 mL ethanol in a mortar. Dilution of the 10 wt % mixture yielded the 1 wt % mixture; dilution of the 20 wt % mixture yielded the 2 wt % and 5 wt % mixtures.

About 5 mg of each mixture prepared above was melted approximately 20 K above its melting point on a coverslip for several minutes to a transparent droplet and quenched to room temperature by contact with an aluminum block. The samples were stored in a capped plastic tube filled with Drierite before XPS analysis. After measurements, the samples remained amorphous and transparent without crystallization.

Differential scanning calorimetry (DSC)

The glass transition of each mixture was measured by a TA Q2000 differential scanning calorimeter. Each sample of 4–7 mg was placed in a crimped aluminum pan. The glass transition temperature $T_{\rm g}$ was measured during heating at 10 K/min after vitrifying a melt by cooling at 10 K/min. All measurements were performed under 50 mL/min N₂ purge.

X-ray photoelectron spectroscopy (XPS)

XPS spectra were measured using a Thermo Scientific K-Alpha X-ray Photoelectron Spectrometer with a monochromic Al K α (1486.6 eV) source. Samples were loaded into a vacuum chamber ($\sim 10^{-5}$ Pa) and measured at room temperature (297 K). An electron flood gun was used to neutralize the surface charge for the non-conductive materials of this work. The spot size of measurement was 400 μ m. A survey scan for all the possible elements was performed at step size of 1 eV and passing energy of 200 eV. High-resolution scans for elements of interest were performed at step size of 0.1 eV step and passing energy of 50 eV. For quantitative measurement of atomic ratios, high-resolution scans were used. XPS spectra were analyzed using the Avantage Data System. Calibration of binding energy was made by shifting the observed carbon peak (C 1s) to 285.0 eV. The baseline for integration was obtained from a smart baseline function in Avantage.

Results and Discussion

XPS method validation. When a solid is irradiated by an X-ray, surface atoms can emit photoelectrons. ²¹ From the energies of the X-ray and the emitted electrons, the binding energy can be calculated for the atoms from which photoelectrons originate. An XPS spectrum is a plot of the photoelectron count against binding energy where each peak corresponds to a specific atom and electronic orbital. ²² Using the Relative Sensitivity Factors (RSF), the photoelectron counts can be converted to the atomic fractions. ²³ Because electrons travel only a short distance through solids, XPS is surface sensitive. The XPS intensity as a function of penetration depth, x, is given by $I = I_0 \exp(-x/\lambda)$, where the decay length λ is approximately 3 nm for photoelectrons originating from nitrogen (N 1s) and oxygen (O 1s) in organic compounds. ^{24, 25} In practice, only photoelectrons from a surface layer less than $3\lambda \approx 9$ nm thick are detected.

Our first task was to validate the XPS method for measuring the surface concentrations of

amorphous drugs. For this purpose, we investigated 10 *pure* compounds for which no surface enrichment or depletion occurs. These compounds are collected in Table 2. Each compound was measured in the form of an amorphous film prepared by melt-quenching; one or two spots were measured in each sample. For each compound, a specific atomic ratio is determined by XPS and compared with the theoretical value from the molecular formula. For example, for APAP, the measured N/O ratio is 0.508 (0.035) and the theoretical ratio is 0.5. The ratio method was adopted to eliminate systematic errors; for example, it avoids the carbon peak that is prone to error from contamination. Table 2 shows that the XPS method accurately determined the atomic ratios, with a mean absolute error of 5 %. In Figure 1,

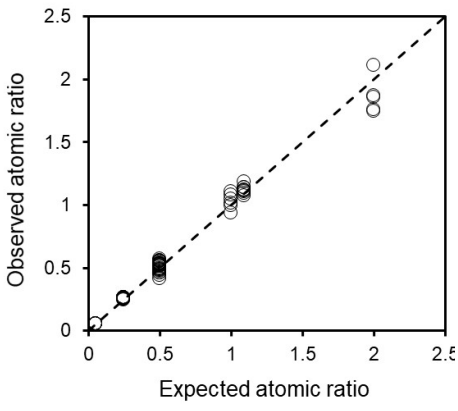


Figure 1. XPS measured atomic ratios plotted against theoretical values for pure compounds in Table 2. The dash line indicates perfect agreement.

the measured and theoretical atomic ratios are plotted against each other, again verifying a close agreement and absence of systematic error.

$T_{-}1.1_{-}2$ VDC		A i A i		- 1 4	P 1
Table / XPS	measured a	itomic ratios ve	expected v	ames 1	for pure compounds

Model drugs	Formula	Ratio	Expected	Observed	Std. dev.	% difference
Acetaminophen	$C_8H_9NO_2$	N/O	0.5	0.508	0.035	1.5
Celecoxib	$C_{17}H_{14}F_3N_3O_2S$	S/O	0.5	0.525	0.014	5.0
Indomethacin	$C_{19}H_{16}ClNO_4$	Cl/O	0.25	0.256	0.006	2.3
Itraconazole	$C_{35}H_{38}Cl_{2}N_{8}O_{4}$	N/O	2	1.867	0.147	-6.6
Ketoconazole	$C_{26}H_{28}Cl_2N_4O_4$	Cl/N	0.5	0.480	0.015	-3.9
Lumefantrine	$C_{30}H_{32}Cl_3NO$	N/O	1	1.033	0.075	3.3
Maltitol	$C_{12}H_{24}O_{11}$	C/O	1.09	1.118	0.031	2.5
Posaconazole	$C_{37}H_{42}F_2N_8O_4$	F/O	0.5	0.529	0.049	5.8
PVP K30 ^a	(C ₆ H ₉ NO) _n	N/O	1	1.017	0.038	1.7

TPD^b	$C_{38}H_{32}N_2$	N/C	0.053	0.053	0.001	1.3
---------	-------------------	-----	-------	-------	-------	-----

^aPVP K30: Polyvinylpyrrolidone K30

Different surfactants in the common host APAP. In this work, we systematically compared the surface concentrations of four surfactants (Span 20, Span 80, Tween 20, and Tween 80; see Scheme 1) in the common host APAP. To prepare for this study, we established by DSC that all four surfactants are miscible with the host in the concentration range investigated (0–10 wt %). Figure 2a shows the typical DSC results for APAP doped with Span 80. We observe a single glass transition in each sample and a continuous shift of the glass transition temperature T_g with surfactant concentration. This indicates surfactant-host miscibility in the bulk. If the components were phase separated, two glass transitions would be observed and the two T_g s would not vary with concentration.²⁶

In Figure 2b, the T_g of each surfactant-APAP system is plotted against the surfactant concentration. The $T_{\rm g}$ of each surfactant is below the ambient temperature. Thus, a decrease of T_g is expected with increasing concentration of the surfactant¹⁰, and this is indeed observed. The decrease of T_g is observed in the entire range investigated (0-20 wt %). This range covers the concentration range used (0-10 wt %) for the surfaceenrichment study, meaning component miscibility in the bulk exists for all our samples. It is intriguing that in Figure 2b, three surfactants approximately fall in one group, while Span 80 separates from the group, showing the smallest decrease of T_g at the same concentration. This could be a consequence of Span 80 being the most lipophilic surfactant of the group (lowest HLB, see Table 1), while APAP is a hydrophilic compound.

Figure 3a shows the typical XPS result for measuring the surface concentration of a surfactant. In this case, the system is APAP doped with Span 80. The pure APAP spectrum has three prominent peaks for carbon (285 eV), nitrogen (400 eV) and oxygen (533 eV).²² The areas of these peaks are related to the surface atomic composition. For pure APAP, we obtain an N/O atomic ratio of $k = 0.508 \pm 0.035$, very close to the formula value of 0.5.

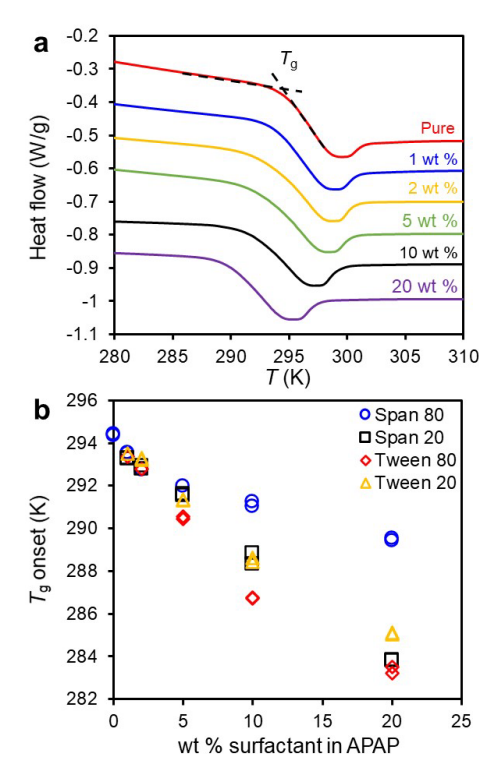


Figure 2. (a) DSC results for Span 80 doped APAP at concentrations indicated. The onset of glass transition temperature $T_{\rm g}$ is indicated. (b) $T_{\rm g}$ vs. surfactant concentration for APAP doped with Span 80, Span 20, Tween 80, and Tween 20.

^bTPD: *N*,*N* '-Bis(3-methylphenyl)-*N*,*N* '-diphenylbenzidine

In the presence of surfactant Span 80 at only 1 wt %, the nitrogen peak diminishes and it almost vanishes at 5 and 10 wt %. This effect is seen more clearly in Figure 3b where only the nitrogen peaks are shown. These peaks have been normalized by the oxygen peaks; that is, these spectra directly report the N/O ratio at the surface. As Span 80 concentration increases, the nitrogen peak decreases. Given that Span 80 has no nitrogen atoms, this result indicates that the surface is significantly covered by Span 80.

Figure 3c shows the nitrogen XPS spectra of amorphous APAP doped with 4 different surfactants: Span 80, Span 20, Tween 80 and Tween 20, all at 5 wt %. In all cases, the nitrogen peak is reduced relative to pure APAP. Since none of these surfactants has nitrogen atoms, this indicates surface enrichment for all the surfactants. We also observe a significant difference between the surfactants: the surface nitrogen peak nearly vanishes in the case of Span 80, but still robust in the other cases. This indicates that the surfactants investigated show different degrees of surface enrichment.

To quantify the surface weight-fraction concentration of a surfactant, w_s , we employ the following equation:

$$w_{S} = \frac{(xk-y)}{M_{d}} / \left[\frac{xk-y}{M_{d}} - \frac{zk}{M_{s}} \right]$$
 (1)

where k is the observed N/O ratio (RSF already applied), x and y are respectively the numbers of oxygen and nitrogen atoms in the drug molecule (x = 2 and y = 1 for APAP), z is the number of oxygen atoms in the surfactant molecule (z = 6 for Span 80), M_d is the molecular weight of the drug, and M_s is the molecular weight of the surfactant. This equation assumes independent responses of atoms in the region probed by the X-ray.

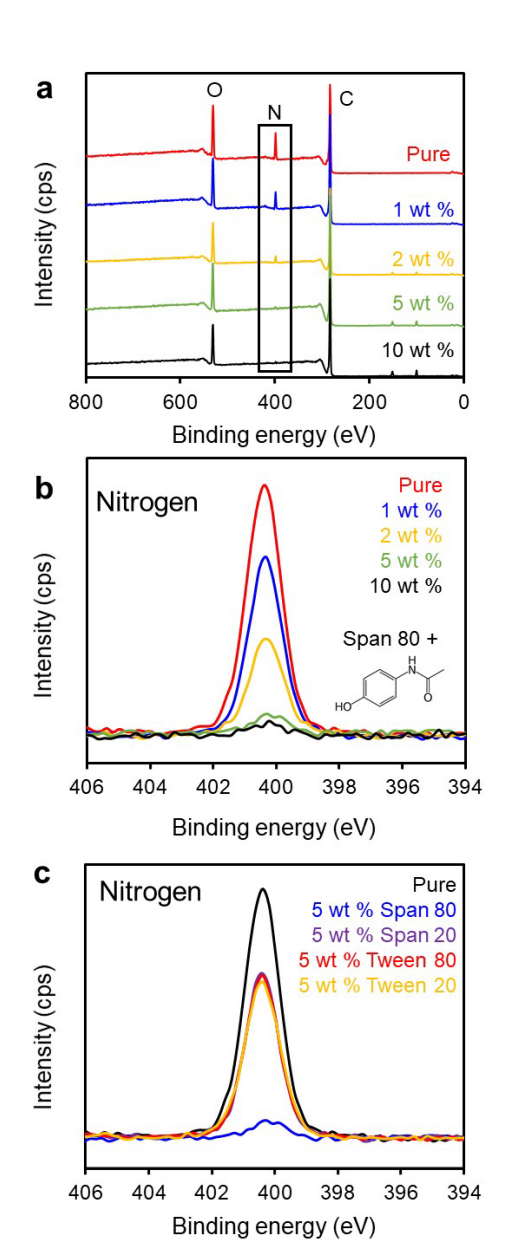


Figure 3. (a) Survey XPS spectra of pure APAP and APAP doped with Span 80 at concentrations indicated. (b) High-resolution scans of the nitrogen peak for samples in (a). (c) High-resolution scans of the nitrogen peak for APAP doped with 5 wt % of different surfactants indicated. In (b) and (c), the intensity has been normalized by the oxygen peak.

Figure 4 shows the surface concentration of each surfactant doped in amorphous APAP as a function of its bulk concentration. The dashed line indicates the condition where surface and

bulk concentrations are equal (no surface enrichment or deletion). We find that *for every surfactant tested, surface concentration is higher than bulk concentration*. The effect is the strongest for Span 80: when the bulk concentration is only 2 wt %, the surface concentration is 50 wt % or 25 times higher; when the bulk concentration is 10 wt %, the surface is nearly pure surfactant (90 wt %). The other three surfactants show weaker but highly significant surface enrichment; for example, at 2 wt % bulk concentration, the surface concentration is 10 times higher on average, at 20 wt %. The different behaviors of the surfactants are consistent with their hydrophilic-lipophilic balance (HLB, see Table 1). Higher HLB means the

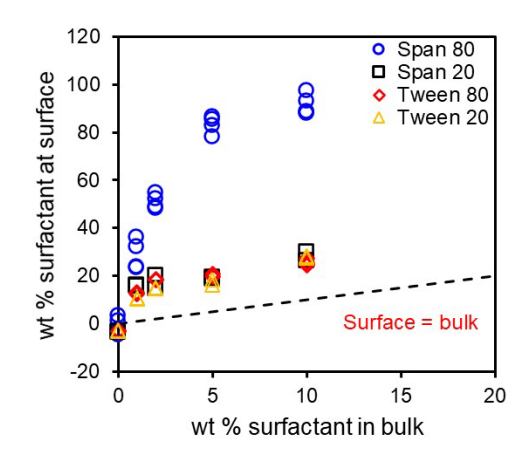


Figure 4. Surface concentration of each surfactant doped in amorphous APAP as a function of its bulk concentration.

surfactant is more hydrophilic on balance. The most lipophilic surfactant Span 80 is expected to have the lowest affinity for the relatively hydrophilic host APAP and show the strongest surface enrichment. It is interesting that despite their different HLB values, Span 20, Tween 80, and Tween 20 have similar degrees of surface enrichment.

Same surfactant Span 80 in different hosts. In this section, we investigate the surface enrichment behavior of the same surfactant Span 80 in several amorphous drugs. As in the case of APAP doped with different surfactants, we first assess component miscibility in the bulk. Figure 5 shows the $T_{\rm g}$ of each surfactant-drug system as a function of surfactant concentration.

We observe that $T_{\rm g}$ generally decreases with surfactant concentration. The concentration range investigated (0–20 wt %) exceeds that used for our surface enrichment study (0–10 wt %), indicating bulk miscibility in all our samples. For ITZ, the decrease of $T_{\rm g}$ is evident up to 10 wt %, but appears to halt between 10 and 20 wt %, suggesting potential immiscibility at higher concentrations. It is interesting that APAP shows the smallest slope of $T_{\rm g}$ decrease with Span 80 concentration. Again, this could arise from the lipophilicity of Span 80 and the hydrophilicity of APAP, leading to a weaker interaction.

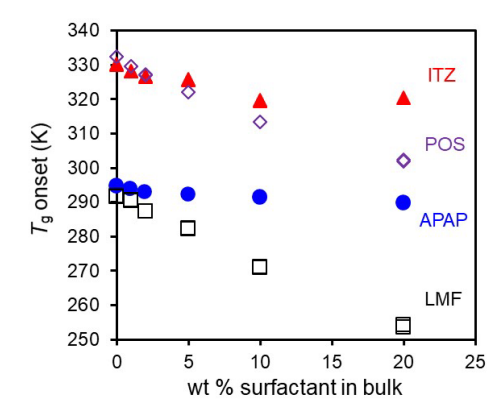


Figure 5. T_g vs. surfactant concentration for Span 80 doped in ITZ, POS, APAP and LMF.

Figure 6 shows XPS spectra of the amorphous drugs doped with Span 80. Since the surfactant contains only carbon and oxygen as heavy atoms, we use drug-specific atoms to quantify the change of surface composition when a surfactant is present. As indicated in Figure 6, the drug-specific atoms are: N for APAP; Cl and N for LMF; F and N for POS; Cl and N for ITZ. An inspection of Figure 6 shows that these peaks decrease in the presence of the surfactant. For example, in the presence of 10 wt % Span 80, the N and Cl peaks of LMF decrease significantly, while the O peak increases, indicating surface coverage by the surfactant. The quantitative changes are calculated using the same method described above. For this purpose, eq. 1 is modified where *k* refers to the X/O ratio, with X being a drug-specific element. When multiple choices of X/O are possible, we use the one whose measured value for the pure compound has the closest agreement with the theoretical ratio. For APAP, LMF and ITZ, N/O is used for this purpose; for POS, F/O is used.

Figure 7a shows the surface concentration of Span 80 in each amorphous drug tested as a function of its bulk concentration. The dashed line indicates the condition of no surface enrichment or depletion. Regardless of the drug matrix tested, Span 80 shows significant surface enrichment. The effect is the strongest in APAP, followed by LMF, POS, and ITZ, though the ranking is ambiguous at some concentrations. In Figure 7b we plot the surface concentration of

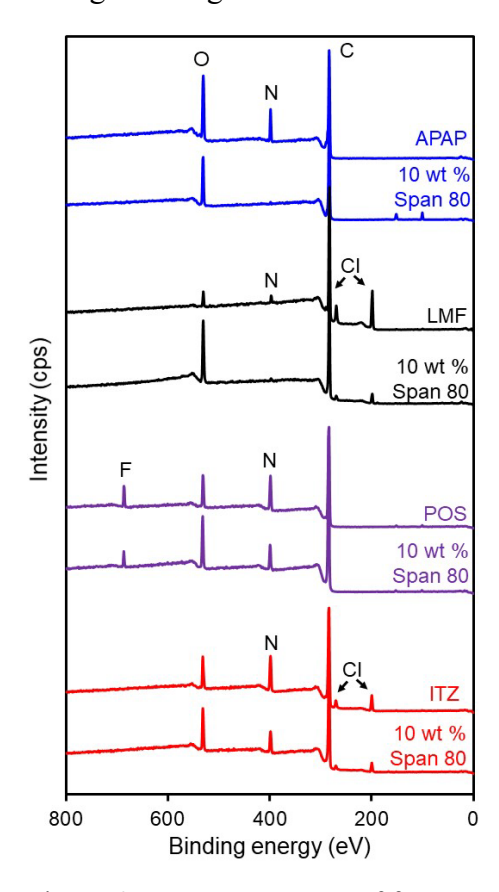


Figure 6. XPS survey scans of four amorphous drugs doped with 10 wt % Span 80. Drug-specific peaks useful for measuring surface concentrations are indicated.

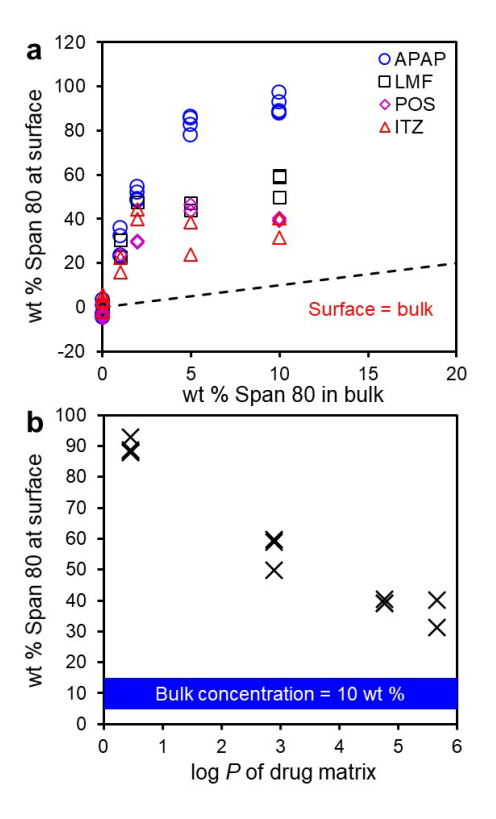


Figure 7. (a) Surface concentration of Span 80 vs. bulk concentration in 4 amorphous drugs. (b) Surface concentration of Span 80 vs. the drug's log *P* at a bulk concentration of 10 wt % (horizontal line).

Span 80 against the drug's $\log P$ with the bulk concentration held constant at 10 wt % (horizontal line). This plot shows a strong correlation between the surface enrichment effect and $\log P$ of the drug, with lower $\log P$ associated with stronger surface enrichment. Thus, for the systems investigated, the degree of surface enrichment increases as the host matrix becomes more hydrophilic. This result is sensible since a more hydrophilic medium should repel more strongly a hydrophobic (lipophilic) component. The most hydrophilic drug of the group (APAP) is thus seen to induce the strongest surface enrichment of Span 80.

Figure 8 presents a schematic summary of the results from this work. We have observed surface enrichment for all surfactants in all the drug matrices tested. The strongest effect was observed with the most lipophilic surfactant Span 80 in the most hydrophilic matrix APAP where a nearly pure surfactant layer is formed at a bulk concentration of 10 wt %. The effect weakens, though still highly significant, with increase of the surfactant hydrophilicity (HLB) and the drug's hydrophobicity. These results are fully consistent with the principle of surface reorganization to minimize surface energy. At a liquid/vapor interface, the hydrophobic tail of a surfactant tends to point toward the vapor while the hydrophilic head points toward the liquid. A more hydrophilic liquid such as APAP promotes this orientation, because it

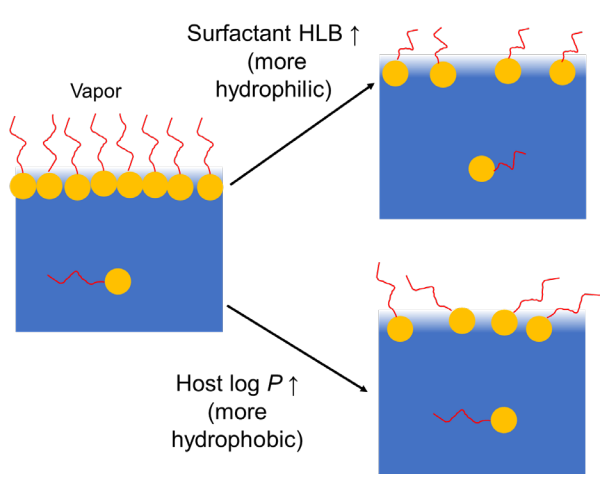


Figure 8. Schematic summary of the results from this work. Surface enrichment occurs in all systems investigated. The effect is strongest for a lipophilic surfactant in a hydrophilic matrix and weakens as the surfactant becomes more hydrophilic and the matrix more hydrophobic.

excludes the surfactant's hydrophobic tails and welcomes contact with its hydrophilic heads. This low-energy configuration drives the formation of a surface layer enriched in the surfactant. As the surfactant molecule becomes more hydrophilic, there is a stronger attractive interaction with the host molecules, reducing the driving force for surface enrichment. This leads to a lower surface concentration of the surfactant molecules. Likewise, as the host liquid becomes more hydrophobic (more lipophilic), the lipophilic tail of the surfactant has higher affinity for the host molecules and there is lower energy penalty to expose the host molecules to the vapor phase. This leads to a lower driving force for the enrichment of surfactant molecules at the liquid/vapor interface.

Conclusions

In this study, we used XPS to measure the surface enrichment effect of surfactants for the first time in amorphous drugs. We investigated four different surfactants (Span 80, Span 20, Tween 80, and Tween 20) in the common host acetaminophen, as well as the same surfactant Span 80 in four different hosts (acetaminophen, lumefantrine, posaconazole, and itraconazole). For each

system, the surfactant concentrations were 0, 1, 2, 5, and 10 wt %, which cover the typical concentration in amorphous formulations, and we confirmed component miscibility in the bulk by DSC. For all systems investigated, we observed significant surface enrichment of the surfactants. For different surfactants doped in acetaminophen, strongest surface enrichment was observed for the most lipophilic Span 80 (lowest HLB). For the same surfactant Span 80 doped in different drugs, the surface enrichment effect increases with the hydrophilicity of the drug (decreasing log *P*). These effects are analogous to the surface enrichment of surfactants in aqueous solutions and fully explained by the principle of surface reorganization to minimize interfacial energy. This study highlights the potentially dramatic difference between surface and bulk concentrations in ASDs.

Surface enrichment of surfactants is expected to impact the stability, wetting, and dissolution of amorphous particles. Given their low $T_{\rm g}$, a high surfactant concentration in the surface region means enhanced local mobility, potentially leading to particle aggregation and accelerated crystallization and chemical degradation. In future work, the surface enrichment effect should be characterized for other components in amorphous formulations (e.g., polymers) and its impact on formulation performance should be better understood. Besides thermodynamic investigations as performed here, it is of interest to determine the kinetics of surface enrichment when a fresh surface is created by fracture.

Acknowledgements

We thank BMS for supporting this work and the NSF-supported University of Wisconsin Materials Research Science and Engineering Center (DMR-1720415) for partial support and the use of its characterization facility.

References

- 1. Yu, L. Amorphous pharmaceutical solids: preparation, characterization and stabilization. *Advanced drug delivery reviews* **2001**, *48*, (1), 27-42.
- 2. Saboo, S.; Bapat, P.; Moseson, D. E.; Kestur, U. S.; Taylor, L. S. Exploring the Role of Surfactants in Enhancing Drug Release from Amorphous Solid Dispersions at Higher Drug Loadings. *Pharmaceutics* **2021**, *13*, (5), 735.
- 3. Ghebremeskel, A. N.; Vemavarapu, C.; Lodaya, M. Use of surfactants as plasticizers in preparing solid dispersions of poorly soluble API: selection of polymer–surfactant combinations using solubility parameters and testing the processability. *International journal of pharmaceutics* **2007**, *328*, (2), 119-129.
- 4. Rasing, T.; Shen, Y.; Kim, M. W.; Valint Jr, P.; Bock, J. Orientation of surfactant molecules at a liquid-air interface measured by optical second-harmonic generation. *Physical Review A* **1985**, *31*, (1), 537.
- 5. Peltonen, L. J.; Yliruusi, J. Surface pressure, hysteresis, interfacial tension, and CMC of four sorbitan monoesters at water—air, water—hexane, and hexane—air interfaces. *Journal of colloid and interface science* **2000**, *227*, (1), 1-6.

- 6. Rodríguez, A.; del Mar Graciani, M.; Angulo, M.; Moyá, M. L. Effects of organic solvent addition on the aggregation and micellar growth of cationic dimeric surfactant 12-3-12, 2Br. *Langmuir* **2007**, *23*, (23), 11496-11505.
- 7. Yu, L. Surface mobility of molecular glasses and its importance in physical stability. *Advanced drug delivery reviews* **2016**, *100*, 3-9.
- 8. Wu, T.; Yu, L. Surface crystallization of indomethacin below T g. *Pharmaceutical research* **2006**, *23*, (10), 2350-2355.
- 9. Powell, C. T.; Xi, H.; Sun, Y.; Gunn, E.; Chen, Y.; Ediger, M.; Yu, L. Fast crystal growth in oterphenyl glasses: a possible role for fracture and surface mobility. *The Journal of Physical Chemistry B* **2015**, *119*, (31), 10124-10130.
- 10. Amim Jr, J.; Blachechen, L. S.; Petri, D. F. Effect of sorbitan-based surfactants on glass transition temperature of cellulose esters. *Journal of thermal analysis and calorimetry* **2012**, *107*, (3), 1259-1265.
- 11. Song, Y.; Zemlyanov, D.; Chen, X.; Su, Z.; Nie, H.; Lubach, J. W.; Smith, D.; Byrn, S.; Pinal, R. Acidbase interactions in amorphous solid dispersions of lumefantrine prepared by spray-drying and hot-melt extrusion using X-ray photoelectron spectroscopy. *International journal of pharmaceutics* **2016**, *514*, (2), 456-464.
- 12. Ton-That, C.; Shard, A.; Daley, R.; Bradley, R. Effects of annealing on the surface composition and morphology of PS/PMMA blend. *Macromolecules* **2000**, *33*, (22), 8453-8459.
- 13. Chen, Z.; Yang, K.; Huang, C.; Zhu, A.; Yu, L.; Qian, F. Surface enrichment and depletion of the active ingredient in spray dried amorphous solid dispersions. *Pharmaceutical Research* **2018**, *35*, (2), 38.
- 14. Sangster, J. LOGKOW databank. *Montreal, Quebec, Canada, Sangster Research Laboratories* **1994**.
- 15. Hussain, S.; Chaudhary, V.; Jain, V.; Khar, R. K.; Yadav, M. Formulation and evaluation of liquid crystalline nanoparticles of combination drugs of antimalarials: Preformulation part.
- 16. Babalola, C. P. Experimental determination of the physicochemical properties of lumefantrine. *African journal of medicine and medical sciences* **2013**, *42*, (3), 209-214.
- 17. Tools, E. A., Models, Estimation Program Interface (EPI) Suite, Version 3.12; US Environmental Protection Agency, Office of Pollution Prevention and Toxics: Washington, DC, 2005. Version.
- 18. O'Neil, M. J.; Smith, A.; Heckelman, P. E. The merck index: An encyclopedia of Chemicals. *Drugs, and Biologicals* **2006**, *13*.
- 19. Dinarvand, R.; Moghadam, S.; Sheikhi, A.; Atyabi, F. Effect of surfactant HLB and different formulation variables on the properties of poly-D, L-lactide microspheres of naltrexone prepared by double emulsion technique. *Journal of microencapsulation* **2005**, *22*, (2), 139-151.
- 20. Hurisso, B. B.; Lovelock, K. R.; Licence, P. Amino acid-based ionic liquids: using XPS to probe the electronic environment via binding energies. *Physical Chemistry Chemical Physics* **2011**, *13*, (39), 17737-17748.
- 21. Hüfner, S., *Photoelectron spectroscopy: principles and applications*. Springer Science & Business Media: 2013.
- 22. Chastain, J.; King Jr, R. C. Handbook of X-ray photoelectron spectroscopy. *Perkin-Elmer, USA* **1992**, 261.
- 23. Wagner, C.; Davis, L.; Zeller, M.; Taylor, J.; Raymond, R.; Gale, L. Empirical atomic sensitivity factors for quantitative analysis by electron spectroscopy for chemical analysis. *Surface and interface analysis* **1981**, *3*, (5), 211-225.
- 24. Seah, M. P.; Dench, W. Quantitative electron spectroscopy of surfaces: A standard data base for electron inelastic mean free paths in solids. *Surface and interface analysis* **1979**, *1*, (1), 2-11.
- 25. Roberts, R.; Allara, D.; Pryde, C.; Buchanan, D.; Hobbins, N. Mean free path for inelastic scattering of 1.2 kev electrons in thin poly (methylmethacrylate) films. *Surface and Interface Analysis* **1980,** *2*, (1), 5-10.

26. Sun, Y.; Tao, J.; Zhang, G. G.; Yu, L. Solubilities of crystalline drugs in polymers: an improved analytical method and comparison of solubilities of indomethacin and nifedipine in PVP, PVP/VA, and PVAc. *Journal of pharmaceutical sciences* **2010**, *99*, (9), 4023-4031.

For Table and Contents Only

